Applied and Environmental Microbiology, May 2011, p. 3017–3023 Vol. 77, No. 9
0099-2240/11/$12.00 doi:10.1128/AEM.01899-10

Specific Electromagnetic Effects of Microwave Radiation on *Escherichia coli*▽

Yury Shamis,[1,2] Alex Taube,[1] Natasa Mitik-Dineva,[1] Rodney Croft,[2,3] Russell J. Crawford,[1] and Elena P. Ivanova[1]*

Faculty of Life and Social Sciences, Swinburne University, Melbourne, Victoria, Australia[1]; Australian Centre for Radiofrequency Bioeffects Research, Melbourne, Victoria, Australia[2]; and School of Psychology, University of Wollongong, Wollongong, New South Wales, Australia[3]

Received 10 August 2010/Accepted 27 February 2011

The present study investigated the effects of microwave (MW) radiation applied under a sublethal temperature on *Escherichia coli*. The experiments were conducted at a frequency of 18 GHz and at a temperature below 40°C to avoid the thermal degradation of bacterial cells during exposure. The absorbed power was calculated to be 1,500 kW/m^3, and the electric field was determined to be 300 V/m. Both values were theoretically confirmed using CST Microwave Studio 3D Electromagnetic Simulation Software. As a negative control, *E. coli* cells were also thermally heated to temperatures up to 40°C using Peltier plate heating. Scanning electron microscopy (SEM) analysis performed immediately after MW exposure revealed that the *E. coli* cells exhibited a cell morphology significantly different from that of the negative controls. This MW effect, however, appeared to be temporary, as following a further 10-min elapsed period, the cell morphology appeared to revert to a state that was identical to that of the untreated controls. Confocal laser scanning microscopy (CLSM) revealed that fluorescein isothiocyanate (FITC)-conjugated dextran (150 kDa) was taken up by the MW-treated cells, suggesting that pores had formed within the cell membrane. Cell viability experiments revealed that the MW treatment was not bactericidal, since 88% of the cells were recovered after radiation. It is proposed that one of the effects of exposing *E. coli* cells to MW radiation under sublethal temperature conditions is that the cell surface undergoes a modification that is electrokinetic in nature, resulting in a reversible MW-induced poration of the cell membrane.

The effects of MW radiation on microorganisms have been studied and debated for more than half a century (3, 4, 10, 12, 17, 20, 28, 29, 35). The nature of the debate surrounding this interaction has often referred to the existence of so-called specific microwave (MW) effects that are nonthermal in nature (4, 10, 13, 17, 20, 28, 29). Much has been published supporting the notion that a range of specific MW effects exist and can be identified in terms of their manifestations on cell physiology (2, 4, 10, 13, 27, 28). For example, Dreyfuss and Chipley examined the effects of MW radiation (2.45 GHz) at sublethal temperatures on the metabolic activities of a range of enzymes expressed by the bacterium *Staphylococcus aureus* (10). These results suggested that MW radiation affected *S. aureus* cells in a way that could not have been explained solely by thermal-effect theories. It has also been found that *Burkholderia cepacia* bacteria could be wholly inactivated using MW radiation at sublethal temperatures at a frequency of 20 GHz (2). Samarketu et al. (25) examined the effects of MW radiation at a frequency of 9.575 GHz on the physiological behavior of *Cyanobacterium dolium* (*Anabaena dolium*). The authors suggested that MW radiation nonthermally induced different biological effects by changing the protein structures by differentially partitioning the ions and altering the rates and/or directions of biochemical reactions (25). It was also suggested that the turbidity of the cell suspension, protein, carbohydrate, chlorophyll *a*, carotenoids, and phycocyanin of microwave-exposed samples were inversely correlated with higher modulation frequencies (25). Previous studies completed by our research group have also demonstrated that sterilization of raw meat (28), as well as transplant biomaterial (27), could be achieved using MW radiation under defined MW settings and solute concentrations. To date, however, no available research has demonstrated a solid understanding of how MW radiation (at a defined range of frequencies) causes certain effects on microorganisms and why they occur.

In light of the paucity of knowledge surrounding the existence of specific MW effects on bacteria, the aim of the present study was to investigate the electromagnetic effects of MW radiation under carefully defined and controlled parameters. *Escherichia coli* cells were processed at sublethal temperatures, and various techniques, including scanning electron microscopy (SEM) and confocal laser scanning microscopy (CLSM), were used to monitor cellular viability, morphology, and membrane permeability following the MW treatment. The theoretical evaluations of the electromagnetic effects of MW radiation on prokaryotic cells and/or cellular membranes were discussed in light of the proposed electrokinetic nature of MW radiation and to confirm experimental observations.

MATERIALS AND METHODS

Bacterial strain, cultivation procedure, and sample preparation. *E. coli* ATCC 15034 was used as a test strain in all experiments. The bacterium was obtained from the American Type Culture Collection. Pure cultures were stored at −80°C in nutrient broth (NB) (Oxoid) supplemented with 20% (vol/vol) glycerol. The bacteria were routinely cultivated for 24 h on nutrient agar (NA), (Oxoid). Working bacterial suspensions were freshly prepared for each independent experiment as described elsewhere (27, 28). The cell density was adjusted to 10^8

* Corresponding author. Mailing address: Swinburne University, Room AS222, AS Building, Burwood Road, Hawthorn, VIC 3122, Australia. Phone: 61392145137. Fax: 61398190834. E-mail: eivanova@swin.edu.au.

▽ Published ahead of print on 4 March 2011.

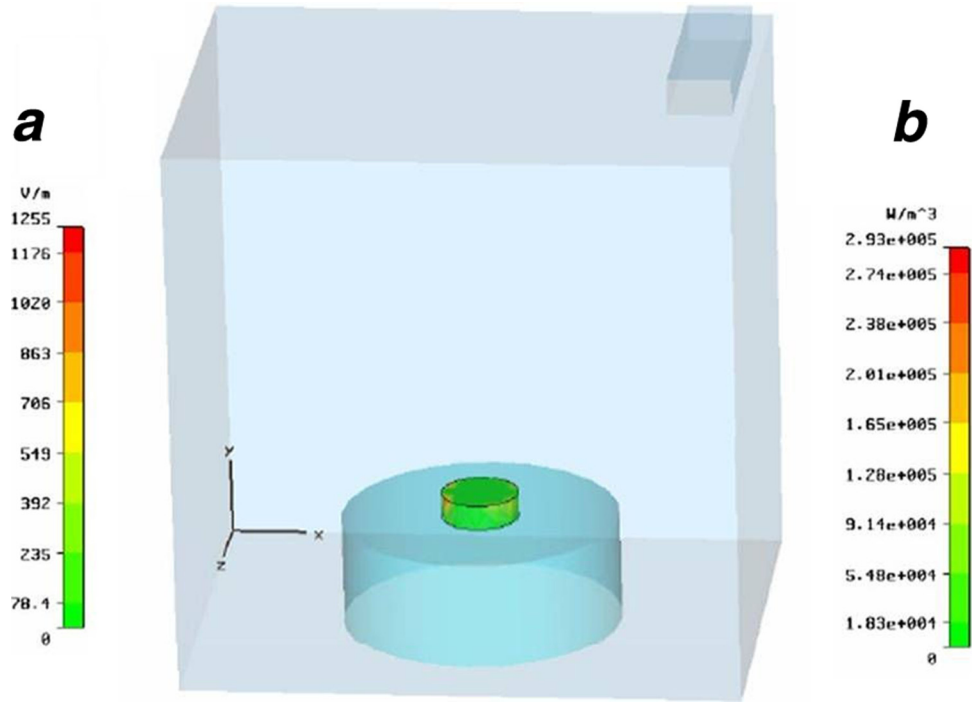

FIG. 1. Modeling using CST Microwave Studio 3D Electromagnetic Simulation Software. (a) Electric field modeling (V/m). (b) Absorbed-power modeling (W/m^3).

CFU per ml (optical density at 600 nm [OD_{600}] = 1.0) in 10 mM phosphate-buffered saline (PBS), pH 7.4, using a spectrophotometer (Amersham Biosciences; Gene Quant Pro) from a bacterial culture grown overnight in 100 ml NB. Bacterial cells were collected during the logarithmic phase of growth as confirmed by growth curves (data not shown). The bacterial cell suspensions were further subjected to direct counting, using a hemocytometer to confirm the number of bacterial cells as described elsewhere (27). Bacterial samples for MW analysis comprised 2 ml of working suspensions that were transferred into a micro-petri dish (35-mm diameter; Griener).

Microwave apparatus. The MW apparatus that was used in the present study had the option of a variable frequency ranging from 5 to 18 GHz (Lambda Technologies; Vari-Wave Model LT 1500). The LT 1500 is a computer-controlled variable-frequency processing cavity for delivering excellent levels of control and uniformity of energy distribution into a multimode microwave cavity. A schematic diagram of the MW apparatus setting has been provided elsewhere (28). Both the amplitude and frequency of the microwave power could be varied, allowing a significant expansion of the parameter space within which the system could be optimized. A data-logging option allowed processed-data capture from the embedded computer system over a standard RS-232-C serial interface. A cavity characterization option was also available, which allowed an evaluation of the performance of material in the cavity to assist in determining the optimum processing conditions.

Microwave settings. Each bacterial sample was transferred into the MW chamber. The chamber had its core temperature monitored through the attachment of a fiber optic probe. In order to minimize thermal MW effects, the bulk temperature rise of the bacterial suspension during exposure was maintained below 40°C, since that was the temperature at which the bacteria were determined to be unaffected by heat. Given that MW frequency is inversely correlated with wavelength, the highest available frequency (18 GHz) was used in all experiments, as it produced the shortest wavelength that is comparable to the bacterial cell diameter and would therefore have the maximum effect on cell kinetics.

For uniformity of exposure, each sample was placed onto a ceramic pedestal (Pacific Ceramics Inc.; PD160; ε' [real part of complex permittivity] = 160; loss tangent $< 10^{-3}$) in the same position in the chamber that had been determined by electric field modeling using CST Microwave Studio 3D Electromagnetic Simulation Software (Fig. 1a).

The experimental apparatus for the MW treatment involved placing the sample in a predetermined location within the MW chamber and subjecting it to a specified radiation treatment at a heating rate of 20°C/min for 1 min, thereby maintaining the temperature rise from 20°C to 40°C. In order to maximize the specific electromagnetic MW effect, a previously optimized "repeated-exposure" technique was employed (27, 28). Each sample was exposed to MW radiation for three consecutive exposures, with the sample allowed to cool to 20°C on ice (at a rate of 10°C per min) between exposures. The temperature profile (by time) is illustrated in Fig. 2.

Thermally heated control samples. In order to ensure that any effects caused by MW radiation were not purely a result of thermal heating, a control sample was used. A Peltier plate heating/cooling system (TA Instruments) was used to replicate the temperature gradients being experienced by the bacteria during MW processing. A total volume of 2 ml of working bacterial suspension was placed onto the Peltier plate and subjected to heating from 20°C to 40°C at a rate of 20°C per min for three consecutive exposures, with cooling times identical to those for MW treatment (at a rate of 10°C per min) between trials (Fig. 2). All experiments using MW-treated samples (in triplicate) were performed in parallel with the Peltier plate-heated samples.

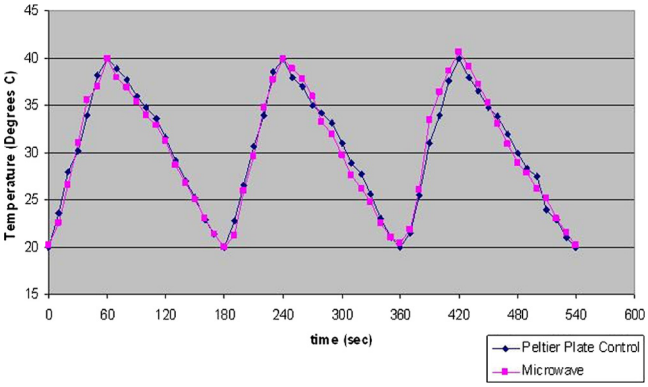

FIG. 2. Temperature profile for the MW-processing system and Peltier plate heating/cooling control.

SEM analysis. A field emission scanning electron microscopy (FeSEM) Zeiss Supra 40VP was used to obtain high-resolution images of the bacterial cells according to a previously developed protocol (27). Primary beam energies of 3 to 15 kV were used, which allowed features on the sample surface or within a few micrometers of the surface, respectively, to be observed.

Immediately following radiation and Peltier plate treatment, 100-μl aliquots of the bacterial suspensions were transferred onto a glass coverslip. Half of the samples were immediately washed with distilled water, air dried (this process took less than 60 s to complete), and then sputter coated with gold prior to being imaged according to a previously developed laboratory protocol (22). The remainder of the samples were left to stand for 10 min and then transferred to a coverslip, washed, dried, and sputter coated. This was performed to identify any changes in cell morphology following exposure to MW radiation and to determine whether these changes were reversible with time. The control for these experiments consisted of 100 μl of untreated bacterial suspension that was transferred onto a glass coverslip, washed with distilled water, air dried, and sputter coated with gold.

Approximately 20 SEM images taken at ×5,000 magnification were analyzed. The recorded densities have estimated errors of approximately 10% due to local variability in the coverage. The number of cells observed from the SEM images prior to and following treatment was transformed into a number of bacteria per unit area, and the percentage of affected cells was calculated accordingly. Statistical data processing was performed using SPSS 16.0 software (SPSS Inc., Chicago, IL).

CLSM analysis. CLSM analysis was performed in order to determine whether the bacterial cell membrane was damaged as a result of MW radiation exposure, thus allowing cell permeability. A fluorescent-dye probe (fluorescein isothiocyanate [FITC]-dextran; 150 kDa; Sigma-Aldrich) was added to the bacterial suspension at a concentration of 25 μg/ml. The bacterial suspensions were then subjected to MW radiation and Peltier plate treatment at the optimized settings. Following radiation and Peltier plate treatment, 1 ml of each suspension was washed twice and resuspended (centrifugation at 5,000 rpm for 3 min and removal of the supernatant). A 20-μl volume of each suspension was then transferred to a glass slide and viewed using an Olympus FluoView FV1000 Spectroscopic Confocal System, which included an inverted Olympus IX81 Microscope System (20×, 40× [oil], and 100× [oil] universal infinity system [UIS] objectives) and operated using multiple Ar and HeNe lasers (458, 488, 515, 543, and 633 nm). The control for these experiments consisted of 1 ml of untreated bacterial suspension mixed with the fluorescent probe and processed simultaneously with the treated bacterial suspensions. Approximately 15 CLSM images were analyzed (5 images per treatment group).

In order to tentatively determine the sizes of the formed pores, an experimental equation (equation 1) that takes into account the radius of the dextran molecule in relation to its molecular weight (14) was used.

$$\text{Radius of dextran molecule (Å)} = 0.33(\text{MM})^{0.46} \tag{1}$$

where MM is molecular mass (Da).

Cell viability. In order to investigate the effects of MW processing on bacterial cell growth/viability, working bacterial suspensions were subjected to MW radiation or Peltier plate treatment. Samples were then diluted to a concentration of approximately 300 CFU/ml as described elsewhere (27), and 100 μl of each suspension was spread onto NA plates and incubated for 36 h at 37°C. The control for these experiments consisted of an untreated bacterial suspension that was processed simultaneously with the treated samples. Evaluation of colony formation (in CFU) and the corresponding statistical analysis were performed as described elsewhere (27, 28).

Theoretical background. This study was designed using accurately controlled experimental conditions and well-defined MW radiation parameters. The modeling of the distribution of the electric field using CST Microwave Studio 3D Electromagnetic Simulation Software allowed us to determine the electrical field absorbed by the sample. This value was estimated to be ~1,500 kW/m^3 (Fig. 1b).

Theoretical calculations were also employed to validate the modeling analysis. Equation 2 depicts a theoretical calculation using the general thermodynamic formula for absorbed power.

$$\frac{P_{\text{Abs}}}{V} = \frac{c\rho\Delta T}{t} \tag{2}$$

where ΔT is the increase in the mean temperature of the heated body; P is microwave power used for heating (in W); V, c, and ρ are volume, heat capacity, and density (in m^3, J/kg × K [kelvin], and kg/m^3); and T is the heating time (in seconds).

Using equation 2, where c is equal to 4.200 J/kg/°C, ρ is equal to 1,000 kg/m^3, ΔT is equal to 20°C, and t is equal to 60 s, the power absorbed by the sample was calculated to be approximately 1,600 kW/m^3. A further calculation was completed to verify the absorbed power in an MW-processing system. The value of the MW power absorbed in the unit volume of the heated load (P_v) is described theoretically in equation 3.

$$P_v = 2 \times \pi \times f \times \varepsilon_0 \times \varepsilon'' |E|^2 \tag{3}$$

where P_v is the power absorbed in the unit volume of the load (in W/m^3), f is the microwave frequency (in Hz), ε_0 is the permittivity of free space (in F/m), ε'' is the dielectric loss factor of the load minus the relative value (1), and E is the strength of the electric field inside the load (in V/m).

By substitution of values, f is equal to 18 GHz, ε_0 is equal to 8.85×10^{-12} F/m, ε'' is equal to 36.34, and E is equal to 300 V/m, and using equation 3, the absorbed power was calculated to be at approximately 1,400 kW/m^3. A comparison of these analyses (absorbed power calculated using equations 2 and 3 and the software simulation) highlighted the consistency between the experimental and modeling results.

Furthermore, it was determined that the total biomass of the bacteria in the suspension was significantly lower than the total mass of water in the suspension and therefore could be taken as negligible for the purposes of modeling calculations. (Multiplying the approximate number of cells in the suspension [0.8×10^8 cells/ml] by the generally accepted average mass of a single *E. coli* cell [9.5×10^{-13} g] [23] indicated that the overall biomass in the bacterial suspension was approximately 1.52×10^{-7} g [in a 2-ml suspension], which could be regarded as an insignificant mass.)

Based on previously reported data regarding the dielectric properties of bacterial cells and organelles (11, 18, 26, 30), it was assumed that the dielectric loss factor of the bacterial sample was lower than that for the surrounding liquid. The heating within a heterogeneous system can be expressed by the ratios of the temperature rise rate:

$$\left[\frac{\Delta T}{\Delta t}\right]_{\text{water}} \div \left[\frac{\Delta T}{\Delta t}\right]_{\text{bacteria}} = \frac{\varepsilon''_{\text{water}}}{\varepsilon''_{\text{bacteria}}} \times \frac{C_{\text{bacteria}}}{C_{\text{water}}} \times \frac{\rho_{\text{bacteria}}}{\rho_{\text{water}}} \tag{4}$$

where $\Delta T/\Delta t$ is the rate of temperature rise, C_{water} is the specific heat capacity (in kJ/kg K) for water and bacteria, and ρ_w and ρ_b are the densities (in kg/m^3) of water and the bacteria.

Thus, the rate of change in temperature of the bacteria would be lower than that for the surrounding liquid. The changes in the dielectric properties during microwave processing was considered insignificant due to the fact that in the temperature interval from 20°C to 40°C, dielectric loss does not change by more than 10% (31).

The average dielectric constant of the bacterial suspension was therefore assumed to be that of water at 18 GHz ($\varepsilon_r = \varepsilon' + j\varepsilon'' = 44 + j36$) (where ε_r is the dimensionless relative complex permittivity and j represents the imaginary unit) (36). Similarly, the specific heat of the total sample was taken as that of water.

In order to determine whether the temperature inside the bacterial cells was the same as that of the surrounding medium, the depth of penetration of MW radiation was also determined using equations 5 to 7. At a frequency of 18 GHz, the wavelength of the microwave in a vacuum was calculated, using equation 3, to be 16.7 mm.

$$\lambda_{18} = \frac{3 \times 10^8 \text{ (m/s)}}{18 \times 10^9 \text{ (liters/s)}} \tag{5}$$

where λ_{18} is the wavelength of the microwave in a vacuum at 18 GHz, m is the length in meters, and s is the time in seconds.

The wavelength in water was determined to be 2.34 mm using equation 6.

$$\lambda_w = \frac{\lambda}{\sqrt{\varepsilon'_r}}\left[\frac{2}{\sqrt{1 + \tan^2\delta} + 1}\right]^{1/2} \tag{6}$$

where λ_{water} is the wavelength of the microwave in water, λ is the wavelength of the microwave in a vacuum (16.7 mm), ε_r' is the static relative permittivity of water ($\varepsilon' = 44$ at 25°C and 18 GHz), and tan δ is the loss tangent (tan δ = 0.821 at 25°C and 18 GHz).

From this calculation, the depth of penetration of microwave radiation into the sample was determined to be 1.04 mm (equation 7).

$$Z = \frac{\lambda}{2\pi}\left[\frac{2}{\varepsilon'(\sqrt{1 + \tan^2\delta} - 1)}\right]^{1/2} \tag{7}$$

where Z is the depth of penetration (power/energy), λ is the wavelength of the microwave in a vacuum, ε_r' is the static relative permittivity of water ($\varepsilon' = 44$ at

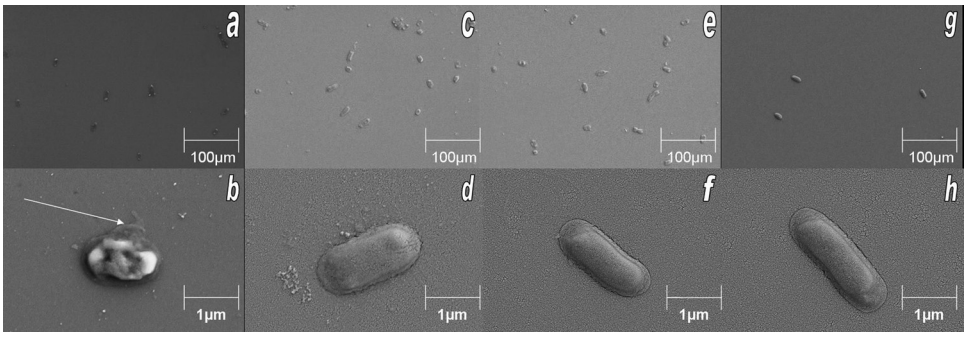

FIG. 3. Typical SEM images of *E. coli*. (a and b) MW-treated cells immediately following radiation. (c and d) Untreated control cells. (e and f) MW-treated cells 10 min after exposure to radiation. (g and h) Thermally heated control cells immediately following Peltier plate treatment. The arrow in panel b indicates leakage of cytosolic fluids out of the *E. coli* cell.

25°C and 18 GHz), and tan δ is the loss tangent (tan δ = 0.821 at 25°C and 18 GHz).

Given that the total depth of the sample in the micro-petri dish was calculated to be 1.00 mm, it was assumed that complete penetration was achieved. In light of the assumptions and calculations, the temperature inside the bacterial cells was suggested to be the same as the temperature in the surrounding medium.

RESULTS AND DISCUSSION

The SEM analysis in the present study revealed that *E. coli* cells that were dried for 60 s following exposure to MW radiation exhibited a cell morphology different than that of all other treatment groups (Fig. 3). As can be seen from the images in Fig. 3a and b, up to 98% ± 1% of the cells had a dehydrated appearance, in contrast to all control groups, where no change in morphology was observed (Fig. 3c to f). Statistical analysis revealed a significant difference between these data: $t(18) = 8.77$; $P < 0.05$ [where t is the ratio of the departure of an estimated parameter from its notional value and its standard error and (18) represents the degrees of freedom].

Cell viability experiments revealed that up to 87.7% ± 4% of MW-treated *E. coli* cells and 89.9% ± 2% of *E. coli* cells after Peltier plate treatment remained viable and were recovered on nutrient agar plates. A statistical analysis of the data revealed that no significant differences existed between the two treatment groups ($P > 0.05$). It can be inferred from these results that the specific MW effect was not bactericidal under the current experimental conditions. The small reduction in bacterial cell numbers following both MW and Peltier plate processing was therefore most likely due to thermal shock. It had been reported previously that even slight increases in temperature can have weak bactericidal effects (4). Our previous studies (27, 28), which accomplished nearly complete bacterial inactivation following exposure to MW radiation, were performed at 45°C, suggesting that by varying certain experimental conditions, such as temperature and/or osmolarity, a diversity of specific MW effects may be manifested.

Our current observations allow us to postulate that the application of MW radiation might cause disruption of the cellular membrane so that the cytosolic fluids within the *E. coli* cells are able to pass through the membrane. This effect, however, appeared to be temporary, as the shape of the cells appears to have recovered within 10 min after the application of MW radiation (Fig. 3c and d). This was most likely due to the reabsorption of the fluids into cells. The morphology of all Peltier plate-treated cells (Fig. 3g and h) examined immediately following treatment appeared unaffected and identical to that of untreated control cells. To our knowledge, no data are currently available regarding the observation of specific effects of MW radiation on the morphology of prokaryotic cells.

Interestingly, however, our findings appeared to be in agreement with the results reported for eukaryotic cells by Chang and Reese (7), who observed the shrinkage of human red blood cells following electroporation caused by the application of a pulsed radiofrequency electric field in a hypo-osmotic medium (notably, a continuous-wave electric field was generated as a result of the MW treatment in the present study). Using SEM, the authors also observed that within 30 s, all cells had swelled back to their original morphology. It was concluded that the shrinkage was the result of a rapid escape of cellular material via pores formed in the membrane (7). The study did not report data pertaining to the resulting cell physiological condition(s).

In order to evaluate whether MW radiation affected the cell membrane integrity and caused pore formation within cellular membranes, high-molecular-mass (150-kDa) FITC-dextran fluorescent probes were used in the present study. Dextran molecules are relatively uncharged and therefore predominantly unaffected directly by the presence of an electric field. This simple assay was used to determine whether pores were formed during MW exposure, thus allowing the free-floating dextran molecules to penetrate the cell membrane during the rehydration process and to remain trapped inside the cell. As can be seen in Fig. 4b, all MW-treated cells appeared to have ingested the dextran molecules, whereas only 17% ± 3% of the untreated controls (Fig. 4a) and 13% ± 4% of the Peltier plate-treated cells (Fig. 4c) appeared fluorescent. A subsequent statistical analysis indicated that there was a significant difference in the number of fluorescent MW-treated cells compared to the thermally heated and untreated controls [$t(13) = 6.34$; $P < 0.05$]. It is proposed that the minor amount of fluorescence observed for the control and Peltier plate-treated cells was most likely a result of cell membrane damage caused by the centrifugation of the cell suspensions.

The size of the dextran probes was calculated to be 15.9 nm. Given that the dextran molecules were able to pass through the cell membrane, it can be concluded that the sizes of pores formed within the *E. coli* cell membrane were equal to or larger than the diameter of each dextran probe, i.e., 15.9 nm. The actual sizes of pores formed within the cell membrane

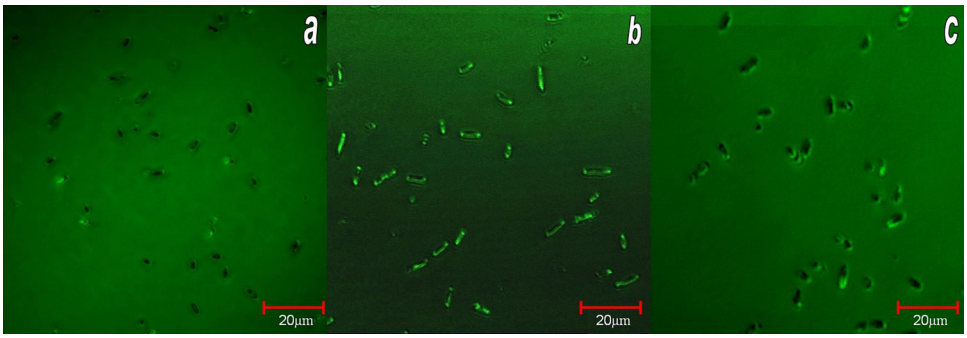

FIG. 4. Typical two-dimensional confocal microscopy images of *E. coli.* (a) Untreated control cells. (b) MW-treated cells. (c) Peltier plate-treated cells.

were not determined in the present study. This finding is consistent with previous pulse-induced reversible electroporation studies, where pore sizes of approximately 11 nm were detected using 70-kDa FITC-dextran probes. Images obtained using rapid-freezing electron microscopy, together with estimations using theoretical models (21), have suggested that pore diameters as large as 120 nm can be induced using electric fields where reversible electroporation occurs. The overall conclusion of this section of the study supported the SEM results, indicating that MW radiation exposure under the specified settings caused reversible MW-induced poration of the *E. coli* cell membrane and that this behavior appeared to be similar to that observed for traditional reversible electroporation processes.

General discussion. The vast majority of the data reported previously has been inferred from experiments completed at temperatures in the range of 45°C to 60°C, which are near or greater than the thermal degradation points of the target organisms, thus making it very difficult, if not impossible, to make a clear distinction between the thermal- and nonthermal-specific effects of MW radiation (19, 35). At these temperatures, protein denaturation and breakdown of cell membrane structures, as well as the disruption of replication machinery, occur (4, 28). While the above-mentioned studies reported different findings when MW was used than when conventional heating methods were used, the results in many of these publications cannot be used for interpreting the heat-independent effects of MW radiation because of the experimental temperatures employed. Furthermore, replication of studies that have suggested the existence of specific MW effects at sublethal temperatures has generally been unsuccessful, due to the great variability in the experimental conditions, such as MW frequency and power and exposure times. It has been shown that the manifestation of specific MW effects on microorganisms has been observed only when particular combinations of these factors are present (3, 4, 27).

The challenge in investigating the specific effects of MW exposure on microorganisms at sublethal temperatures involves the inherent difficulty in measuring the temperature of a sample during microwave processing and the inaccuracies in measurement that can result. The first source of inaccuracy is the presence of an uneven electric field distribution inside the microwave cavity. The microwaves within the enclosed cavity experience numerous reflections and produce a constructive-destructive interference pattern within the cavity that creates localized "hot spots." A hot spot is a thermal irregularity that arises because of the nonlinear dependence of the electromagnetic and thermal properties of the material on temperature. This effect leads to nonuniform power absorption by the sample, which in turn leads to nonuniform heating and temperature distribution within the sample. In the present study, this effect was diminished by placing the sample on a ceramic pedestal that made the field distribution relatively even. This arose from the dielectric properties of the ceramic block, which allowed the concentration of the electric field around the sample, causing a uniform power distribution throughout the sample. Furthermore, as the calculated wavelength of microwaves in the cavity (2.34 mm) was much greater than the dimensions of each bacterial cell, the possibility of uneven heating due to nonuniform field distribution was negligible.

Since the cell morphology following Peltier plate heating appeared identical to that of the control, it can be assumed that the specific effect of MW radiation was due to a direct electromagnetic interaction with the bacterial cells. In the experiments reported in this study, such direct electromagnetic interactions affected the cellular membrane, causing the reversible development of cell membrane pores accompanied by the leakage of cytosolic fluids through these pores. This observation has led to the suggestion that a possible specific effect of MW radiation at sublethal temperatures on bacteria is similar to that of electroporation of the cell membrane. Electroporation is the production of pores in a cell membrane by the application of transverse electric fields (32). It has been determined from observations of substances being transported into and out of cells (24), freeze fracture studies (7), and measurements determining the change in membrane impedance after direct-current treatment of cells (16) that electroporation allows normally nonpermeant matter to diffuse freely through the membranes (34). While the exact mechanisms by which the electrical pulses cause the cell membrane to be permeabilized are not yet fully understood, it is thought that the electric field causes localized structural rearrangements within the cell membrane (32), resulting in the formation of pores that allow the free transport of ionic and molecular material through the cell wall (33). Depending on the field strength and exposure time, the subsequent removal of the electric field may then allow the cell membrane to regain its structural integrity (8).

Analysis of the SEM images obtained for *E. coli* in the present study, the visual reversibility of the MW effect, and the

uptake of fluorescent dextran probes in MW-treated cells suggests that under current experimental conditions MW radiation caused reversible MW-induced poration whose morphological manifestation was similar to that observed in traditional electroporation using pulsed fields. Electromagnetic fields in the MW frequencies are known to significantly increase the conductivity and permeability of materials (5), particularly due to enhanced diffusion (1) and enhanced mobility of ions (6). In comparison to traditional electroporation caused by direct currents, high-frequency electromagnetic fields amplify all of the kinetic processes, unlike low-frequency fields. This is because ions cross the cell membrane under two influences: diffusion and the application of an electric field (9). High-frequency electromagnetic fields, which change the direction of ion movement at an approximate rate of 10^{10} times per second, enhance both of these effects.

This study is, to the best of our knowledge, the first of its kind to provide evidence of the reversible leakage of cellular cytosolic fluids and a visual representation of the morphological changes occurring in *E. coli* cells following exposure to continuous-wave MW radiation at sublethal temperatures. Given that electro-osmosis occurred as a result of the pores formed by the exposure to MW radiation, the MW–bacterial-cell interaction was described as electrokinetic in nature. An electrokinetic phenomenon, in particular electro-osmosis, refers to a motion of liquid in a porous body under the influence of an electric field (15). We propose that molecular transport caused by the MW radiation is controlled by electrokinetic mechanisms that increase transport rates, i.e., a dynamic interaction of the microwave field and the cell involving both membrane charging and discharging controls electrical behavior and molecular transport. The important role of electrokinetics is supported by the analyses based on electrohydrodynamic theory and our numerical simulations and experimental results. Further detailed investigations are required to more fully understand the mechanisms by which microwaves interact with bacterial cells. A study of the extent of pore formation and pore size within the cell membrane as a result of MW exposure will be required before this technique can be used in industrial and biomedical applications.

In summary, the results of this study indicate that the interaction of continuous-wave MW radiation at sublethal temperatures with bacteria appears to be electrokinetic in nature. Temporary changes in cell morphology and the uptake of fluorescent probes suggest that during MW treatment pores are formed within the bacterial cell membrane. The observed reversibility of the dehydration effect, together with the lack of bactericidal effects, suggests that this treatment method has the potential to be applied to a range of bioindustrial and biomedical applications.

ACKNOWLEDGMENT

We thank Peter Cadusch for his comments and discussion of the manuscript.

REFERENCES

1. **Antonio, C., and R. T. Deam.** 2007. Can "microwave effects" be explained by enhanced diffusion? Phys. Chem. Chem. Phys. **9:**2976–2982.
2. **Arndt, D., et al.** 2005. Microwave radiation: therapeutic application for cure of subcutaneous bacterial infections. Space Life Sciences. NASA Biennial Research and Technology Report. National Aeronautics and Space Administration, Houston, TX.
3. **Atmaca, S., Z. Akdag, S. Dasdag, and S. Celik.** 1996. Effect of microwaves on survival of some bacterial strains. Acta Microbiol. Immunol. Hung. **43:**371–378.
4. **Banik, S., S. Bandyopadhyay, and S. Ganguly.** 2003. Bioeffects of microwave: a brief review. Bioresour. Technol. **87:**155–159.
5. **Bober, K., R. H. Giles, and J. Waldman.** 1997. Tailoring the microwave permitivity and permeability of composite materials. Int. J. Infrared Millimeter Waves **18:**101–123.
6. **Challis, L. J.** 2005. Mechanisms for interaction between RF fields and biological tissue. Bioelectromagnetics **26:**S98–S106.
7. **Chang, D. C., and T. S. Reese.** 1990. Changes in membrane structure induced by electroporation as revealed by rapid freezing electron microscopy. Biophys. J. **58:**1–12.
8. **Chen, C., J. A. Evans, M. P. Robinson, S. W. Smye, and P. O'Toole.** 2008. Measurement of the efficiency of cell membrane electroporation using pulsed AC fields. Phys. Med. Biol. **53:**4747–4757.
9. **Despa, S.** 1995. The influence of membrane permeability for ions on cell behaviour in an electric alternating field. Phys. Med. Biol. **40:**1399–1409.
10. **Dreyfuss, M. S., and J. R. Chipley.** 1980. Comparison of effects of sublethal microwave radiation and conventional heating on the metabolic activity of *Staphylococcus aureus*. Appl. Environ. Biol. **39:**13–16.
11. **Foster, K. R., and H. P. Schwan.** 1995. Dielectric properties of tissue. p. 37–96. *In* C. Polk and E. Postow (ed.), Handbook of biological effects of electromagnetic fields, vol. 2. CRC Press, Boca Raton, FL.
12. **Fujikawa, H., H. Ushioda, and Y. Kudo.** 1992. Kinetics of *Escherichia coli* destruction by microwave irradiation. Appl. Environ. Microbiol. **58:**920–924.
13. **George, D. F., M. M. Bilek, and D. R. McKenzie.** 2008. Non-thermal effects in the microwave induced unfolding of proteins observed by chaperone binding. Bioelectromagnetics **29:**324–330.
14. **Granath, K., and B. Kwist.** 1967. Molecular weight distribution analysis by gel chromatography on sephadex. J. Chromatogr. **28:**69–81.
15. **Haynie, D. T.** 2001. Biological thermodynamics, vol. 2. Cambridge University Press, Cambridge, United Kingdom.
16. **Huang, Y., and B. Rubinsky.** 2000. Micro-electroporation: improving the efficiency and understanding of electrical permeabilization of cells. Biomed. Microdevices **2:**145–150.
17. **Hyland, G. J.** 1998. Non-thermal bioeffects induced by low-intensity microwave irradiation of living systems. Eng. Sci. Ed. J. **7:**261–269.
18. **Jeng, D. K., K. A. Kaczmarek, A. G. Woodworth, and G. Balasky.** 1987. Mechanism of microwave sterilization in the dry state. Appl. Environ. Microbiol. **53:**2133–2137.
19. **Kim, S. Y., E. K. Jo, H. J. Kim, K. Bai, and J. K. Park.** 2008. The effects of high-power microwaves on the ultrastructure of Bacillus subtilis. Lett. Appl. Microbiol. **47:**35–40.
20. **Kozempel, M., R. D. Cook, O. J. Scullen, and B. A. Annous.** 2000. Development of a process for detecting non-thermal effects of a microwave energy on microorganisms at low temperature. J. Food Proc. Preservation **24:**287–301.
21. **Krassowska, W., and P. D. Filev.** 2007. Modelling electroporation in a single cell. Biophys. J. **92:**404–417.
22. **Mitik-Dineva, N., et al.** 2009. Differences in colonisation of five marine bacteria on two types of glass surfaces. Biofouling **25:**621–631.
23. **Neidhardt, F. C., J. L. Ingraham, and M. Schaechter.** 1990. Physiology of the bacterial cell: a molecular approach. Sinauer Associates Inc., Sutherland, MA.
24. **Neumann, E., and K. Rosenheck.** 1972. Permeability changes induced by electric impulses in vesicular membranes. J. Membrane Biol. **10:**279–290.
25. **Samarketu, S. P., S. P. Singh, and R. K. Jha.** 1996. Effect of direct modulated microwave modulation frequencies exposure on physiology of cyanobacterium *Anabena dolilum*, p. 155–158. *In* Proceedings of the Asia Pacific Microwave Conference, vol. 2. IEEE, Piscataway, NJ.
26. **Sanchis, A., et al.** 2007. Dielectric characterization of bacterial cells using dielectrophoresis. Bioelectromagnetics **28:**393–401.
27. **Shamis, Y., et al.** 2009. A new sterilization technique of bovine pericardial biomaterial using microwave radiation. Tissue Eng. C Methods **15:**445–454.
28. **Shamis, Y., et al.** 2008. Development of a microwave effect for bacterial decontamination of raw meat. J. Food Eng. **4:**1–15.
29. **Shazman, A., S. Mizrahi, U. Cogan, and E. Shimoni.** 2007. Examining for possible non-thermal effects during heating in a microwave oven. Food Chem. **103:**444–453.
30. **Stuchly, M., and S. Stuchly.** 1990. Electrical properties of biological substances, p. 75–112. *In* O. P. Gandhi (ed.), Biological effects and medical applications of electromagnetic energy. Prentice Hall, Englewood Cliffs, NJ.
31. **van der Veen, M. E., A. J. van der Goot, C. A. Vriezinga, J. W. G. De Meester, and R. M. Boom.** 2004. On the potential of uneven heating in heterogeneous food media with dielectric heating. J. Food Eng. **63:**403–412.
32. **van Uitert, I., S. Le Gac, and A. V. D. Berg.** 2010. The influence of different membrane components on the electrical stability of bilayer lipid membranes. Biochim. Biophys. Acta **1798:**21–31.
33. **Weaver, J. C.** 2003. Electroporation of biological membranes from multicellular to nano scales. IEEE Trans. Dielectrics Electrical Insulation **10:**754–768.
34. **Weaver, J. C., and Y. A. Chizmadzhev.** 1996. Theory of electroporation: a review. Bioelectrochemistry **41:**135–160.
35. **Woo, I. S., I. K. Rhee, and H. D. Park.** 2000. Differential damage in bacterial cells by microwave radiation on the basis of cell wall structure. Appl. Environ. Microbiol. **66:**2243–2247.
36. **Zaghloul, H., and H. A. Buckmaster.** 1985. The complex permittivity of water at 9.356 GHz from 10 to 40 degrees C. J. Phys. D Appl. Phy. **18:**2109–2118.